

Received June 16, 2020, accepted June 27, 2020, date of publication July 14, 2020, date of current version July 24, 2020.

Digital Object Identifier 10.1109/ACCESS.2020.3009276

# Deep Semantic Segmentation and Multi-Class Skin Lesion Classification Based on Convolutional Neural Network

MUHAMMAD ALMAS ANJUM<sup>1</sup>, JAVARIA AMIN<sup>2</sup>,  
MUHAMMAD SHARIF<sup>3</sup>, (Senior Member, IEEE), HABIB ULLAH KHAN<sup>4</sup>, (Member, IEEE),  
MUHAMMAD SHERAZ ARSHAD MALIK<sup>5</sup>, AND SEIFEDINE KADRY<sup>6</sup>, (Senior Member, IEEE)

<sup>1</sup>College of Electrical and Mechanical Engineering, National University of Sciences & Technology (NUST), Islamabad 46000, Pakistan

<sup>2</sup>Department of Computer Science, University of Wah, Wah 46000, Pakistan

<sup>3</sup>Department of Computer Science, COMSATS University Islamabad, Wah Campus, Wah 47040, Pakistan

<sup>4</sup>Department of Accounting and Information System, College of Business & Economics, Qatar University, Doha, Qatar

<sup>5</sup>Department of Information Technology, Government College University Faisalabad, Faisalabad 38000, Pakistan

<sup>6</sup>Department of Mathematics and Computer Science, Faculty of Science, Beirut Arab University, Beirut 11072809, Lebanon

Corresponding authors: Muhammad Sharif (muhammadsharifmalik@yahoo.com) and Habib Ullah Khan (habib.khan@qu.edu.qa)

This work was supported by the Qatar University Internal Grant under Grant IRCC-2020-009.

**ABSTRACT** Skin cancer is developed due to abnormal cell growth. These cells are grown rapidly and destroy the normal skin cells. However, it's curable at an initial stage to reduce the patient's mortality rate. In this article, the method is proposed for localization, segmentation and classification of the skin lesion at an early stage. The proposed method contains three phases. In phase I, different types of the skin lesion are localized using tinyYOLOv2 model in which open neural network (ONNX) and squeeze Net model are used as a backbone. The features are extracted from depthconcat7 layer of squeeze Net and passed as an input to the tinyYOLOv2. The propose model accurately localize the affected part of the skin. In Phase II, 13-layer 3D-semantic segmentation model (01 input, 04 convolutional, 03 batch-normalization, 03 ReLU, softmax and pixel classification) is used for segmentation. In the proposed segmentation model, pixel classification layer is used for computing the overlap region between the segmented and ground truth images. Later in Phase III, extract deep features using ResNet-18 model and optimized features are selected using ant colony optimization (ACO) method. The optimized features vector is passed to the classifiers such as optimized (O)-SVM and O-NB. The proposed method is evaluated on the top MICCAI ISIC challenging 2017, 2018 and 2019 datasets. The proposed method accurately localized, segmented and classified the skin lesion at an early stage.

**INDEX TERMS** YOLOv2, ant colony optimization, squeeze Net, ResNet-18, SVM, ONNX.

## I. INTRODUCTION

Skin cancer is a more aggressive and common in human beings. It's caused due to abnormal cells growth. These cells are developed through mitosis and replicate themselves. Melanoma is caused due to anomalous cell growth; these cells replicate themselves by migrating from bloodstream to other body organs and also infect the adjacent skin tissues. The basement membrane provides protection for epidermis. Cancerous cells grow and bypass the basement membrane and spread into the inner skin layers. Melanocytes create

brown pigment known as melanin. Melanin is a protective pigment, which provides protection to the skin from ultra-violet rays. Skin cancer is commonly caused to those peoples who play or work outside and it is typical amongst sunbathers. Fair-skinned peoples are mostly affected by skin cancer due to less melanin production. However, skin cancer may also develop in dark skinned people, due to lack of exposure to sunlight [1]. From 2008- 2018 current news depicted that, 53% rise in new melanoma cases are diagnosed yearly [2], [3]. In the next 10 years the death rate of this disease is estimated to increase. If treated in later stages, less than 14% survival rate of this disease [4], [5]. Therefore, diagnosis of skin cancer at an earlier stage is necessary

The associate editor coordinating the review of this manuscript and approving it for publication was Shuihua Wang<sup>id</sup>.

and a challenging task. The classified dermatologists mostly pursues a sequence of steps for skin cancer diagnosis, first of all they do observation of suspected lesions with an naked eye, then microscopically magnifying lesions and monitored by biopsy. This is a time-consuming task and the patients are diagnosed too far ahead. Depending on the ability of the clinician, correct diagnosis/treatment is subjective. Dermatologists diagnose the skin lesion having accuracy less than 80% [6]. In health care centers, there are not many professional doctors available all around the world. Therefore computerized methods are implemented so far for detection of the skin cancer [7]. The machine learning algorithms such as decision tree [8] Bayesian classifiers [9], and SVM [10] are used to classify different grades of the skin cancer. However, accurate skin cancer detection still a intricate task due to several factors such as variability in texture, shape, color and size of the lesion, poor contrast/brightness, light/dark hairs, and irregular/unclear lesion boundaries. The optimized features extraction/selection is also a challenging task for accurate classification [11]. To overcome these challenging tasks, this article investigates a new methodology for the detection of eight types of skin cancer such as MN, BCC, AK, NV, BKL, DF, VL, and SCC. The foremost contribution steps are opted for accurate detection is as follows:

- YOLOv2-SqueezeNet model is used for localization of the infected region with locations, class label as well as prediction scores.
- The localized affected region is segmented using modified 13-layers semantic segmentation model.
- Deep features are extracted and selected using ResNet-18 and ACO respectively. The resultant features vector is passed to the O-SVM and O-NB for skin lesions classification.

## II. RELATED WORK

Recently much work is carried out for discrimination of different kinds of skin lesions, some of which are discussed in this section [12]. Skin lesions are detected in four major steps i.e., preprocessing, segmentation, features extraction and finally classification. During image acquisition, dermoscopic images having certain artifacts such as thin/thick hair, low contrast image resolution, dark spots/bubbles around the infected skin region and irregular lesion boundary that ultimately minimize accuracy of skin lesion detection. To handle these challenging tasks preprocessing help in accurate detection of the skin lesion [13]. The high pass filter is used to highlight the edges; further illumination is removed by homomorphic filter [14]. Segmentation is a crucial step, provides significant information about lesion such as border, shape, asymmetry and the irregularity [15]. Morphological filtering with weight based features selection approach is used for detection of lesion boundary [16]. Star shape semantic segmentation method is used for skin lesion segmentation [17]. ABCD rule-based approach is used for skin lesion detection. In which total dermoscopic scores are also measured on the basis of asymmetry, lesion diameter and color [18].

Feature extraction is a third major step to extract meaningful information from the input images based on the certain characteristics such as shape, color and texture. However, best features selection is also a challenge for improved classification [18]. Hence after GLCM features extraction, GA is applied for the selection of optimum features [19]. PCA and PSO are also used for the selection of active features vectors [20]. After features extraction, classification is done to discriminate the affected skin region into benign/malignant. The KNN, decision tree [21] and SVM [22] are used for skin lesions classification. Deep learning methods [23]–[25] are mostly utilized for skin lesions detection [2]. Esteva et al developed GoogLeNet and Inception V3 CNN models for skin cancer classification. AlexNet [26] model is applied on the dermoscopic images to learn the pattern of the skin lesion. The extracted features pattern in the form of vector is passed to the multiclass SVM for discrimination among the healthy and infected skin region. Deep full resolution convolution network (DFRCN) with softmax layer [27] is used for classification of skin lesion.

## III. PROPOSED METHODOLOGY

The proposed deep learning approach for skin lesion detection as shown in Fig 1, where ONNX [28] and squeeze Net [29] models are used as backbone of the YOLOv2 [30] model to localize the skin lesions more accurately. The semantic segmentation model is trained based on ground truth annotations to perform pixel wise classification. Later deep features are extracted using ResNet-18 model. The optimized features are selected using ACO which passed to the O-SVM [31] and O-NB [32] classifiers.

### A. LOCALIZATION OF SKIN LESIONS

YOLOv2-squeezeNet model is proposed for localization of the actual skin lesions. In this model, pre-trained squeezeNet is used as a backbone of the open neural network (ONNX) model. The squeezeNet contains 68 layers such as 01 input, 26 convolutional, 26 ReLU, 03 maxpooling, 08 depth concatenation, 01 drop out, 01 average pooling, softmax and classification. The input images size of  $300 \times 300 \times 3$  are used to train the network. The features are extracted from depth concatenation 'fire7-concat' layer of the squeezeNet model and passed as an input to the YOLOv2. YOLOv2-squeezeNet is trained on the selected hyperparameters as mentioned in Table 1.

TABLE 1. YOLOv2-SqueezeNet configuration parameters.

Number of Classes	08
Anchors	[43 59 18 22 23 29 84 109]
Rate of learning	0.001
Size of mini-batch	16
Number of Epochs	200
Verbose Frequency	30

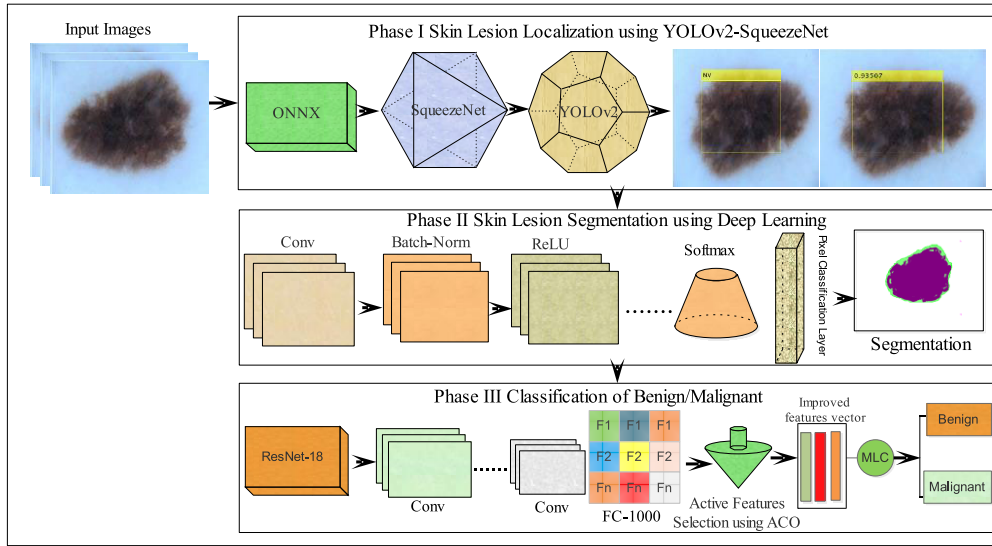


FIGURE 1. Proposed model architecture where MLC denote Machine learning classifier).

YOLO loss is computed into three major categories such as localization, confidence and classification. Localization loss computes the error between actual and predicted bounding box. While, confidence loss is measured through addition of the confidence scores when skin lesions are detected and when it is not detected in a bounding box of a grid cell. Wherease, classification loss compute squared error among conditional class probabilities for each class in the grid cell. The YOLO loss function is computed as shown below:

$$\begin{aligned}
 \text{Loss} = & A_1 \sum_{i=0}^{G^2} \sum_{j=0}^B 1_{ij}^{\text{Malignant}} \left[ (x_i - \hat{x}_i)^2 + (y_i - \hat{y}_i)^2 \right] \\
 & + A_1 \sum_{i=0}^{G^2} \sum_{j=0}^B 1_{ij}^{\text{Malignant}} \\
 & \times \left[ \left( \sqrt{w_i} - \sqrt{\hat{w}_i} \right)^2 + \left( \sqrt{h_i} - \sqrt{\hat{h}_i} \right)^2 \right] \\
 & + A_2 \sum_{i=0}^{G^2} \sum_{j=0}^B 1_{ij}^{\text{Malignant}} (s_i - \hat{s}_i)^2 \\
 & + A_3 \sum_{i=0}^{G^2} \sum_{j=0}^B 1_{ij}^{\text{Benign}} (s_i - \hat{s}_i)^2 \\
 & + A_4 \sum_{i=0}^{G^2} 1_i^{\text{Malignant}} \sum_{c \in \text{classes}} (p_i(c) - \hat{p}_i(c))^2
 \end{aligned} \tag{1}$$

where, G, B, h, w, p, and s denotes number of grid cells, number of the bounding box, height, width, probability, and confidence scores, respectively. The localization and classification losses are controlled using weight parameters A<sub>1</sub> and A<sub>4</sub>, respectively. Similarly, A<sub>2</sub> and A<sub>3</sub> control the confidence loss.

The variable with hat denote ground truth value in i<sup>th</sup> grid cell. Whereas, the variable without hat and subscript i represent value of j<sup>th</sup> bounding box in i<sup>th</sup> grid cell. (x<sub>i</sub>, y<sub>i</sub>) and (x̂<sub>i</sub>, ŷ<sub>i</sub>) represent the center points of j<sup>th</sup> bounding box and

ground truth with respect to i<sup>th</sup> grid cell, respectively. Skin lesions are localized using proposed YOLOV2-squeezeNet as shown in the Fig 2.

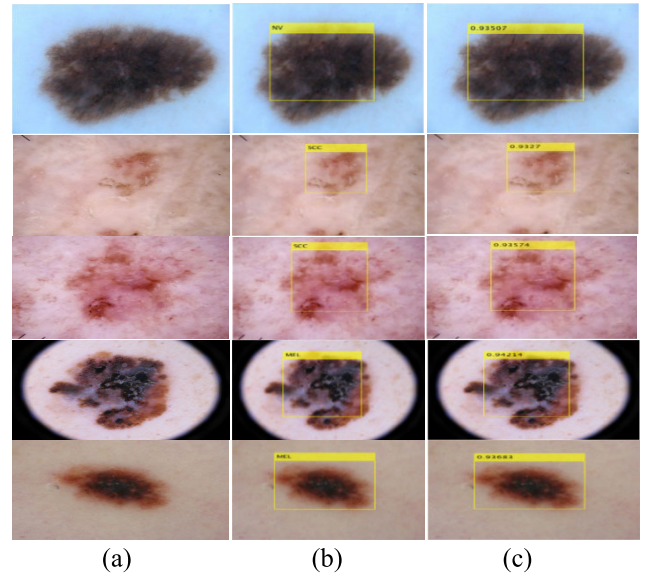


FIGURE 2. Localization results (a) input images (b) localized with class labels (c) localized with predicted scores.

### B. SEGMENTATION OF SKIN LESIONS

In this work, 13-layer semantic segmentation model is proposed. The segmentation model consists of four blocks that are illustrated in Figure 3.

The dilated convolution layer might increase receptive field of layer without increase the number of the parameters or the computations. Therefore, in this model, two dilation convolution layers having dilation factor 1 and 2 are used.

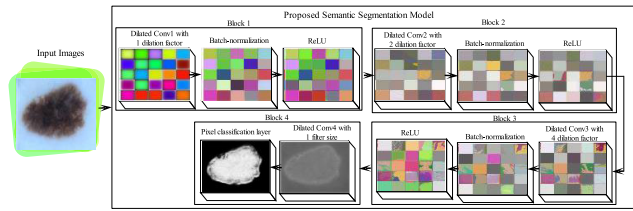


FIGURE 3. Proposed semantic segmentation model with activation units.

In which  $3 \times 3$  filter size convolutional layer and pads the input size is same to the output size through setting [1111] padding option.

Two batch-normalization layers are used among the convolution and the ReLU layers to normalize the input  $x_i$  by measuring the  $\mu_B$  and  $\sigma_B^2$  over the mini-batch size to speed up the CNN training and also minimize the sensitivity of the network initialization.

The normalize activations are defined as:

$$\hat{x}_i = \frac{x_i - \mu_B}{\sigma_B^2 + \epsilon} \quad (2)$$

In the decoder section dilated convolution layer with 4 dilated factors is used. The last convolutional layer is applied with  $1 \times 1$  filter size to squeeze down the number of channels related to the class labels. The mini-batch size of the proposed model is 16. The model is trained on maximum 300 epochs, with  $1e-3$  learning rate. The layered architecture of the segmentation model for training is mentioned in Table 2. The segmented lesion region is shown in Fig 4.

TABLE 2. Layered Architecture of the segmentation model.

Layer	Activation
Input image	$300 \times 300 \times 3$
Convolutional 1	$300 \times 300 \times 32$
Batch-normalization 1	$300 \times 300 \times 32$
ReLU1	$300 \times 300 \times 32$
Convolutional 2	$300 \times 300 \times 32$
Batch-normalization 2	$300 \times 300 \times 32$
ReLU2	$300 \times 300 \times 32$
Convolutional 3	$300 \times 300 \times 32$
Batch-normalization 3	$300 \times 300 \times 32$
ReLU3	$300 \times 300 \times 32$
Convolutional 4	$300 \times 300 \times 2$
Softmax	$300 \times 300 \times 2$
Pixel classification	-

### C. CLASSIFICATION OF DIFFERENT KINDS OF SKIN LESIONS

In medical domain, different types of disease classification using machine learning approaches are helpful for medical

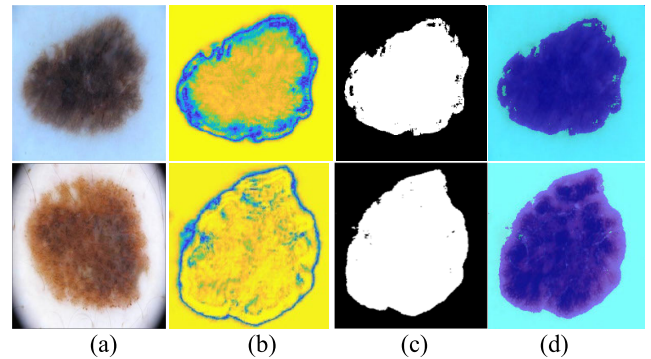


FIGURE 4. Shows lesion segmentation (a) input images (b) contour (c) binary segmentation (d) annotated lesion region.

specialists. The computerized approaches more computationally exhaustive due to increase the number of the patients slices. The deep convolutional neural networks perform better on large number of the input data as compared to classical methodologies [33]. In deep learning methodologies, features are extracted from input and integrated into single matrix to improve the performance. In this article, ResNet-18 model is applied for features extraction. The ResNet-18 model consists of 71 layers such as 01 input, 20 convolutional, 20 batch-normalization, 17 ReLU, 08 addition, 01 maxpooling, 01 average pool, fully connected (FC), softmax and classification. The extracted features are mapped using cross-entropy activation function that is defined as:

$$H_C(f_i, L) = - \sum_C P_{(o,L)} \text{LOG}(P_{(o,L)}) \quad (3)$$

where P denote probability, f shows features vector, L represent class labels, o denote observation over the class.

Cross-entropy activation function is applied separately on training and testing images. The training and testing ratio is selected 50/50 that return two features vectors as output. Later active deep features are selected using ACO. The active selected features vector  $f_i$  fed to the O-SVM and O-NB for classification of different categories of the skin disease. The features extraction/selection process for classification is visually presented in the Fig 5.

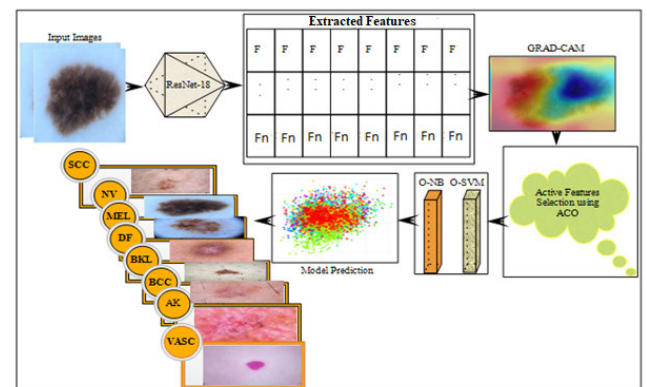


FIGURE 5. Classification using selected extracted features.

**D. FEATURES ENGINEERING AND CLASSIFICATION**

The features vectors are obtained in the previous section, in which prominent features selection from the pool of the features vectors is a challenging task. Therefore in this article features engineering is performed based on ant colony optimization [34]. ACO is a computational approach is utilized for problem optimization. In which problem is optimized by finding shortest path based on the phomone and heuristic exponential weights. The features vector length 1000 is passed to the ACO to find out the active deep features based on optimized cost function. In this approach features are optimized using selected parameters as mention in Table 3. The best cost function is graphically shown in Fig 6.

**TABLE 3. Parameters of ACO.**

Maximum iterations	20
Ants (size of population)	10
Phromone initial	1
Exponential weight phromone	$\alpha=1$
Exponential weight heuristic	$\beta=1$
Rate of Evaporation	$\rho = 0.05$

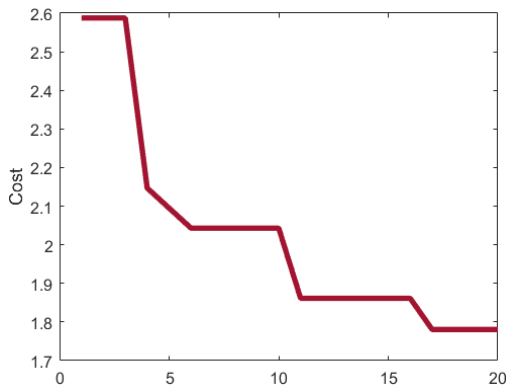


**FIGURE 6. Best cost function using ACO.**

Later optimized features vector is passed to the O-SVM and O-NB classifiers. The selected classifiers are optimized on 30 epochs for model training as graphically shown in Fig 7.

**IV. MATERIAL FOR PERFORMANCE EVALUATION**

The proposed method performance is evaluated on three latest challenging ISIC 2017 [35], 2018 [36] and 2019 [37] datasets. ISBI 2017 dataset having 2,750 images with two classes (2233 benign and 517 malignant).

The ISIC 2018 segmentation dataset contains 12,500 images with ground truth annotations. ISBI classification dataset contains 10,015 images with seven skin cancers classes such as Dermatofibroma (Der), Nevus(Nev), Melanoma(Mel), Pigmented Benign(Pig-Be), Keratoses(Ker), Pigmented Bowen’s(Pig-Bo), Vascular and

Basal Cell Carcinoma (BCC). ISBI 2019 dataset contains 25,331 images with 08 classes such as MN, BCC, AK, BKL, NV, DF, VL, and SCC. In this work ISBI 2019 training data is used for classification of the different types of the skin lesions. The ISIC 2020 dataset contains 33,126 training images of up to 2000 patients with 2 different classes such as benign and malignant [38]. The description about the dataset is mentioned in the Table 4.

**TABLE 4. ISBI 2019 dataset description.**

Types of the skin lesions	Total slices	Total slices after rotation
Melanocytic (MEL)	4522	4522
NV	12875	12875
BCC	3323	3232
AK	867	3470
BKL	2624	3200
DF	239	3232
VASC	253	2240
SCC	628	3200
Total number of images	<b>25331</b>	<b>35971</b>

In Table 4, second column shows total skin lesion slices that are already available in dataset. To increase the size and complexity of dataset, the rotation is applied with different angles such as 30°, 60°, 90°, 120°, 180°, and 270°. In this process we observe that number of images of MEL and NV are sufficient as compared to other types of the lesions. Therefore, we used number of images of MEL and NV without augmentation for experimentation. The 25331 slices are available but after the rotation with different angles numbers of slices are increased up to 35971. Three experiments are implemented to compute the proposed method performance on MATLAB 2020a toolbox with 740K Nvidia Graphic Card.

**A. EXPERIMENT #1 LOCALIZATION OF THE SKIN LESIONS**

In this experiment, YOLOv2-squeezeNet model is applied to localize the skin lesions with class labels as well as predicted scores. The model performance is evaluated with different performance measures such as average precision, Recall, IoU and average log miss rate (am) as mentioned in the Table 5.

**TABLE 5. Performance evaluation of the proposed localization method.**

ISIC Datasets	mAP	am	IoU
2017	0.95	0.50	0.92
2018	0.96	0.40	0.93
2019	1.00	0.00	0.94
2020	0.94	0.60	0.91

The localization results in the Table 5 shows that, methods achieved mAP of 0.95 on ISBI 2017, 0.96 on ISBI 2018, 1.00 on ISBI 2019 and 0.94 on ISIC 2020 datasets. The graphical representation of the mAP with respect to am and IoU is shown in the Fig 8.

The localization results with respect to the class labels and predicted scores are also visually shown in the Figure 9.

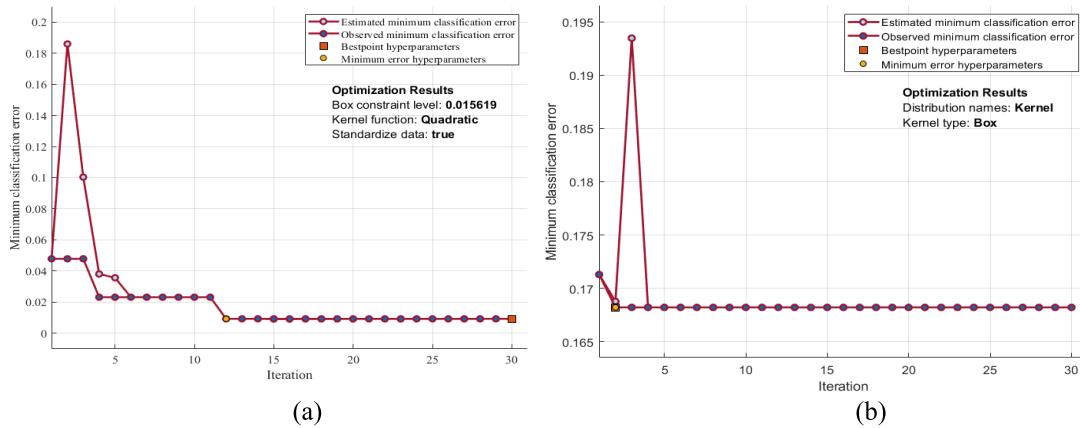


FIGURE 7. Graphically representation of classifiers training (a) O-SVM (b) O-NB.

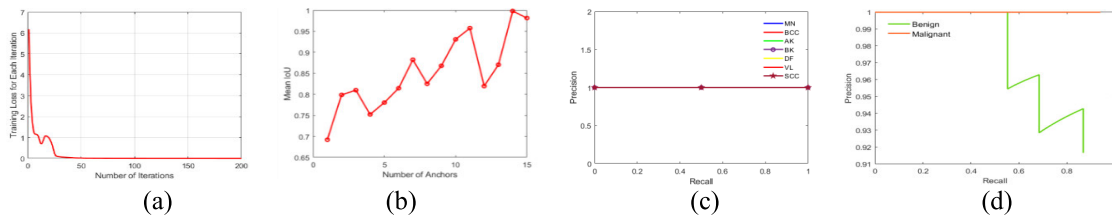


FIGURE 8. Graphically representation of the localization results (a) training loss (b) mean IoU/number of anchors (c) mAP of 8 classes of the skin lesions (d) mAP of two classes (benign and malignant).

**B. EXPERIMENT #2 PIXEL BASED CLASSIFICATION**

In this experiment, localized infected region is segmented using proposed segmentation model. The segmentation results are also evaluated with pixel by pixel with ground truth annotations in term of performance measures such as IoU, and accuracy as mentioned in Table 6.

TABLE 6. Segmentation results of the proposed method.

Dataset	Global ACC	Mean ACC	IoU (Mean)	IoU (Weighted)	BF Score (Mean)
ISBI 2017	0.93	0.94	0.80	0.83	0.85
ISBI 2018	0.95	0.92	0.87	0.86	0.89

The segmentation result in Table 6 shows that, a proposed segmentation method achieves global accuracy of 0.93 on ISBI 2017 and 0.95 on ISBI 2018. Whereas, in this experiment, mean accuracy of 0.94 and 0.92 on ISBI 2017-2018 datasets respectively. The segmented skin lesions are visually shown in Fig 10.

**C. EXPERIMENT #3 CLASSIFICATION OF DERMOSCOPIC IMAGES INTO DIFFERENT CATEGORIES**

This experiment is performed to classify the skin lesions into different categories such as AK, MEL, SCC, BCC, BKL, NV, VL, and DF. In this experiments deep features

vectors are extracted by cross entropy activation function using ResNet-18 model. The optimum features are selected using ACO. The selected features vector is obtained after applying the ACO, fed to machine learning classifiers with 0.5 hold out cross-validation approach. The proposed method classify the input images into benign/malignant on ISBI2017, 2020 datasets, 7 and different categories on ISBI-2018, ISBI-2019 datasets respectively. The classification results with corresponding classes are plotted in the form of confusion matrix as shown in Figure 11.

The discrimination outcomes are computed using different metrics as mentioned in the Table 7-15.

TABLE 7. Classification results on ISBI-2017 using O-SVM.

Total accuracy 97.8%				
Classes	ACC	PPV	Recall/Sensitivity	F1Score
Benign	97.89%	0.99	0.98	0.98
Malignant	97.89%	0.96	0.98	0.97

TABLE 8. Classification results on ISBI-2017 using O-NB.

Total accuracy 99.1%				
Classes	ACC	PPV	Recall	F1Score
Benign	99.03%	1.0	0.99	0.99
Malignant	99.03%	0.98	0.99	0.99

The classification results in Table 7-15, shows that, proposed method classifies the input images into two classes

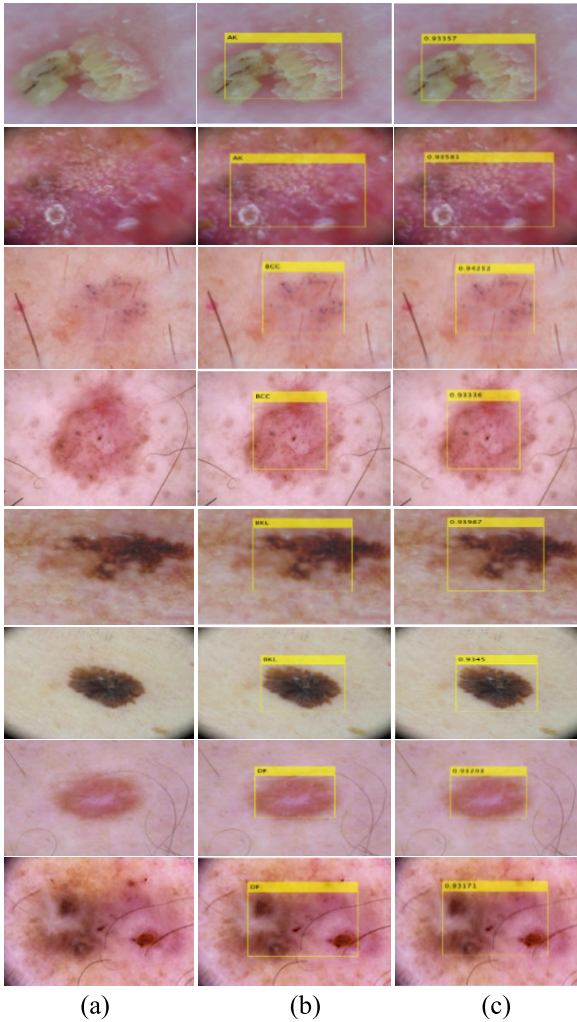


FIGURE 9. Localization of different types of skin lesions (a) input images (b) localized lesion region (c) predicted scores.

TABLE 9. Classification results on ISBI-2018 using O-SVM.

Total accuracy 97.9%				
Classes	ACC	PPV	Recall	F1Score
Der	99.09%	0.97	0.98	0.97
Nev	99.96%	1.0	1.0	1.0
Mel	99.64%	1.0	0.98	0.99
Pig- Be	98.81%	0.97	0.95	0.96
Ker	99.13%	0.95	0.96	0.96
Pig- Bo	99.21%	0.96	0.98	0.97
BCC	99.96%	1.0	1.0	1.0

benign and malignant on ISBI 2017, ISIC 2020 datasets, however, it classify the images into seven and eight classes on ISBI 2018 and 2019 datasets respectively.

The proposed method result in term of accuracy is 97.8%, 99.1% on ISBI 2017 dataset and 99.07%, 83.18% on ISIC 2020 dataset using O-SVM and O-NB respectively. Similarly, 97.9% and 98% accuracy achieved on ISBI 2018 dataset

TABLE 10. Classification results on ISBI-2018 using O-NB.

Total accuracy 98 %				
Classes	ACC	PPV	Recall	F1Score
Der	99.3%	0.95	0.98	0.97
Nev	99.93%	1.0	1.0	1.0
Mel	99.51%	1.0	0.98	0.99
Pig- Be	98.95%	0.98	0.97	0.98
Ker	99.23%	0.94	0.96	0.95
Pig- Bo	99.16%	0.95	0.97	0.96
BCC	99.93%	1.0	0.99	1.0

TABLE 11. Classification results on ISBI 2019 using O-SVM.

Total accuracy 98.1%				
Classes	ACC	PPV	Recall	F1Score
AK	99.52%	0.98	0.99	0.99
BCC	99.82%	1.0	0.99	0.99
BKL	99.85%	1.0	0.99	1.0
DF	99.36%	0.98	0.98	0.98
MEL	99.44%	0.99	0.97	0.98
NV	99.66%	0.99	0.97	0.98
SCC	99.39%	0.95	0.97	0.96
VASC	99.55%	0.96	1.0	0.98

TABLE 12. Classification results on ISBI 2019 using O-NB.

Total accuracy 97.1%				
Classes	ACC	PPV	Recall	F1Score
AK	99.51%	0.98	0.99	0.99
BCC	99.8%	1.0	0.98	0.99
BKL	99.4%	1.0	0.97	0.98
DF	99.32%	0.98	0.97	0.98
MEL	99.02%	0.96	0.97	0.96
NV	99.59%	0.98	0.97	0.97
SCC	99.38%	0.95	0.97	0.96
VASC	99.56%	0.96	1.0	0.98

TABLE 13. Classification results on ISIC-2020 using O-SVM.

Total accuracy 99.07%				
Classes	ACC	PPV	Recall/Sensitivity	F1Score
Benign	99.07%	1.0	0.98	0.99
Malignant	99.07%	0.98	1.0	0.99

TABLE 14. Classification results on ISIC-2020 using O-NB.

Total accuracy 83.18%				
Classes	ACC	PPV	Recall	F1Score
Benign	83.18%	0.89	0.83	0.86
Malignant	83.18%	0.74	0.83	0.78

using O-SVM and O-NB classifiers. The 98.1% and 97.1% accuracy is achieved on ISBI-2019 dataset using O-SVM and O-NB classifiers respectively.

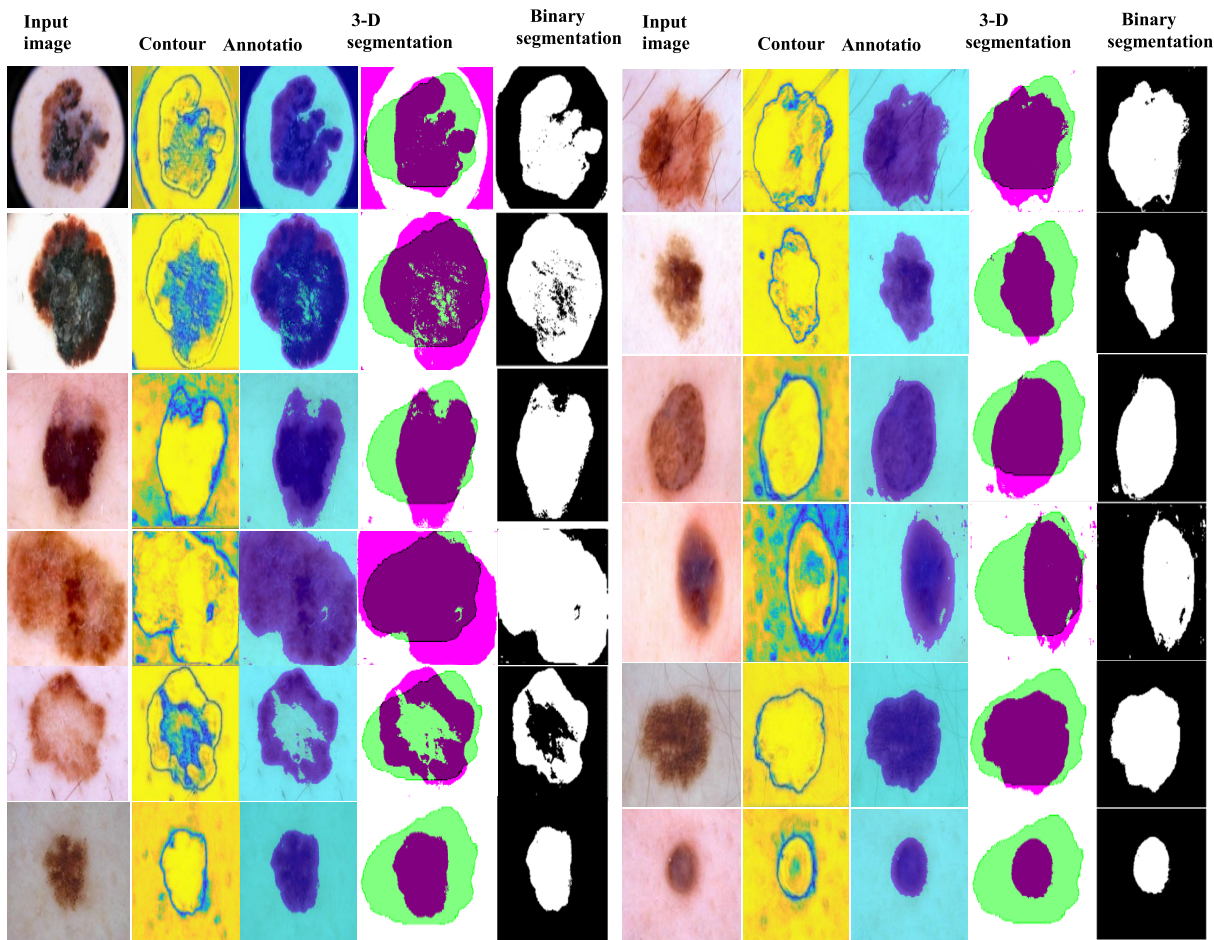


FIGURE 10. Proposed method segmentation results.

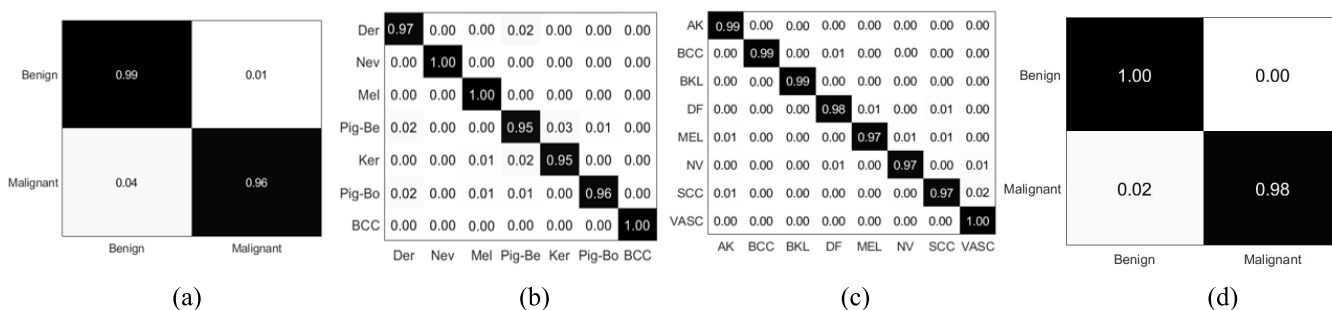


FIGURE 11. Confusion matrix (a) ISBI 2017 (b) ISBI 2018 (c) ISBI 2019 (d) ISIC 2020.

The quantitative results comparison is performed with existing works in term of different performance metrics as mentioned in Table 15.

The classification results compared recent work [39]–[43]. The focus net model is utilized for segmentation, in which encoding layers encode the data properly that helps in the prediction of lesion segmentation. However, focus Net has less sensitive for lesion detection with 0.76 sensitivity [39]. Unet with FCN8s method is used for lesion

segmentation with 0.87 sensitivity and 0.95 specificity on ISIC 2017 dataset [40]. Similarly, ensemble approach, in which combination of the transfer learning models are used for segmentation of the skin lesions with 0.76 validation score [41]. Another existing method used pre-trained model i.e., DenseNet-201, ResNet-50, Inception-v3, Inception-ResNet-v2 models with are used with FrCN for detection of the skin lesions with 0.88 accuracy [42]. Transfer learning models such as VGG16, Densenet201, InceptionResNetV2,



TABLE 15. Existing method comparison.

Ref	Dataset	Year	Results
[39]	ISBI 2017	2019	76% Sensitivity
[40]		2020	87% Sensitivity, 95% Specificity
[41]	ISBI 2018	2019	0.76 Validation score
[42]		2020	88% Accuracy
[43]	ISBI 2019	2020	94.92% Accuracy
<b>Proposed Method</b>			99.1% Accuracy on ISBI 2017, 98.0% Accuracy on ISBI 2018 and 98.1% on ISBI 2019 Accuracy

Google net is used for skin lesion detection on ISBI 2019 dataset with 94.92% accuracy [43].

In this work, two proposed end to end deep models i.e., YOLOv2-SqueezeNet and 3-D semantic segmentation model are fine-tune by the selected configuration parameters that provide accurate localization and segmentation of lesion region. Furthermore, data augmentation is implemented to balance the slices of the different kinds of lesions. After data augmentation, deep features are extracted using cross entropy function and optimum features are selected using ACO. The data augmentation approach with optimized features vector provides higher classification accuracy. The proposed method achieves up to 98% accuracy on ISBI 2018, 2019 and 99% accuracy on ISBI 2017 datasets.

The results comparison, prove that proposed work performed better as compared to latest work published.

## V. CONCLUSION

In this research, ensemble CNN models are proposed for skin lesion detection. In the localization method, ONNX and squeeze Net model is used as a backbone of the YOLOv2 model. In addition, depthconcat7 layer is passed as an input to YOLO model. The method localizes the infected skin lesion more accurately. The method achieves mAP of 0.95, 0.96, 1.00 and 0.94 on ISBI 2017, ISBI 2018, ISBI 2019 and ISIC 2020 datasets respectively. The 3D-segmentation method is also proposed based on CNN. The configuration parameters of the segmentation model are selected after the extensive experiment for accurate lesion segmentation. The segmentation method achieves Global Accuracy of 0.93, 0.95 on ISBI 2017, and ISBI 2018 respectively. The skin lesion classification is performed by applying ResNet-18 model and deep features are extracted by cross entropy activation function. Later, extracted features vectors are enhanced by using ACO method. The hybrid classification approach provides good classification results compared to the recent existing work. In future this work, further enhance to apply the re-enforcement learning for accurately classify the skin lesion.

## ACKNOWLEDGMENT

The findings achieved herein are solely the responsibility of the authors.

## REFERENCES

- [1] W. H. Freeman, "The surgeon general's call to action to prevent skin cancer," US Dept. Health Hum. Services, Office Surgeon Gen., Washington, DC, USA, Rep. Surgeon Gen., 2014.
- [2] A. Esteva, B. Kuprel, R. A. Novoa, J. Ko, S. M. Swetter, H. M. Blau, and S. Thrun, "Dermatologist-level classification of skin cancer with deep neural networks," *Nature*, vol. 542, no. 7639, pp. 115–118, Feb. 2017.
- [3] A. Masood and A. Al-Jumaily, "Computer aided diagnostic support system for skin cancer: A review of techniques and algorithms," *Int. J. Biomed. Eng.*, vol. 2013, pp. 1–22, Dec. 2013.
- [4] B. Erkol, R. H. Moss, R. J. Stanley, W. V. Stoecker, and E. Hvatum, "Automatic lesion boundary detection in dermoscopy images using gradient vector flow snakes," *Skin Res. Technol.*, vol. 11, no. 1, pp. 17–26, Feb. 2005.
- [5] J. Ferlay, M. Colombet, I. Soerjomataram, C. Mathers, D. M. Parkin, M. Piñeros, A. Znaor, and F. Bray, "Estimating the global cancer incidence and mortality in 2018: GLOBOCAN sources and methods," *Int. J. Cancer*, vol. 144, no. 8, pp. 1941–1953, 2019.
- [6] R. Marks, "Epidemiology of melanoma. Clinical dermatology. Review article," *Clin. Exp. Dermatol.*, vol. 25, no. 6, pp. 459–463, Nov. 2000.
- [7] C. Ananth and M. J. Therese, "A survey on melanoma: Skin cancer through computerized diagnosis," *Int. J. Adv. Res. Innov. Discoveries Eng. Appl.*, vol. 5, no. 1, pp. 9–18, Feb. 2020.
- [8] R. Javed, M. S. M. Rahim, T. Saba, and A. Rehman, "A comparative study of features selection for skin lesion detection from dermoscopic images," *Netw. Model. Anal. Health Informat. Bioinf.*, vol. 9, no. 1, p. 4, Dec. 2020.
- [9] Y. Kang, Y. Fang, and X. Lai, "Automatic detection of diabetic retinopathy with statistical method and Bayesian classifier," *J. Med. Imag. Health Informat.*, vol. 10, no. 5, pp. 1225–1233, May 2020.
- [10] M. Li, C. Han, and F. Fahim, "Skin cancer diagnosis based on support vector machine and a new optimization algorithm," *J. Med. Imag. Health Informat.*, vol. 10, no. 2, pp. 356–363, Feb. 2020.
- [11] K. Korotkov and R. Garcia, "Computerized analysis of pigmented skin lesions: A review," *Artif. Intell. Med.*, vol. 56, no. 2, pp. 69–90, Oct. 2012.
- [12] R. B. Oliveira, J. P. Papa, A. S. Pereira, and J. M. R. S. Tavares, "Computational methods for pigmented skin lesion classification in images: Review and future trends," *Neural Comput. Appl.*, vol. 29, no. 3, pp. 613–636, Feb. 2018.
- [13] P. Mehta and B. Shah, "Review on techniques and steps of computer aided skin cancer diagnosis," *Procedia Comput. Sci.*, vol. 85, pp. 309–316, Jan. 2016.
- [14] Q. Abbas, I. F. García, and M. Rashid, "Automatic skin tumour border detection for digital dermoscopy using a new digital image analysis scheme," *Brit. J. Biomed. Sci.*, vol. 67, no. 4, pp. 177–183, Jan. 2010.
- [15] T. K. Lee, "Measuring border irregularity and shape of cutaneous melanocytic lesions," Ph.D. dissertation, Simon Fraser Univ., Burnaby, BC, Canada, 2001.
- [16] G. Schaefer, M. I. Rajab, M. Emre Celebi, and H. Iyatomi, "Colour and contrast enhancement for improved skin lesion segmentation," *Computerized Med. Imag. Graph.*, vol. 35, no. 2, pp. 99–104, Mar. 2011.
- [17] Z. Mirikharaji and G. Hamarneh, "Star shape prior in fully convolutional networks for skin lesion segmentation," in *Proc. Int. Conf. Med. Image Comput. Comput.-Assist. Intervent.* Canada: Springer, 2018, pp. 737–745.
- [18] R. Kasmi and K. Mokrani, "Classification of malignant melanoma and benign skin lesions: Implementation of automatic ABCD rule," *IET Image Process.*, vol. 10, no. 6, pp. 448–455, Jun. 2016.
- [19] M. Sharif, J. Amin, M. Raza, M. Yasmin, and S. C. Satapathy, "An integrated design of particle swarm optimization (PSO) with fusion of features for detection of brain tumor," *Pattern Recognit. Lett.*, vol. 129, pp. 150–157, Jan. 2020.
- [20] T. Y. Tan, L. Zhang, S. C. Neoh, and C. P. Lim, "Intelligent skin cancer detection using enhanced particle swarm optimization," *Knowl.-Based Syst.*, vol. 158, pp. 118–135, Oct. 2018.

- [21] A. Murugan, S. A. H. Nair, and K. P. S. Kumar, "Detection of skin cancer using SVM, random forest and kNN classifiers," *J. Med. Syst.*, vol. 43, no. 8, p. 269, Aug. 2019.
- [22] X. Yuan, Z. Yang, G. Zouridakis, and N. Mullani, "SVM-based texture classification and application to early melanoma detection," in *Proc. Int. Conf. IEEE Eng. Med. Biol. Soc.*, Aug. 2006, pp. 4775–4778.
- [23] C. Kang, X. Yu, S.-H. Wang, D. S. Guttery, H. M. Pandey, Y. Tian, and Y.-D. Zhang, "A heuristic neural network structure relying on fuzzy logic for images scoring," *IEEE Trans. Fuzzy Syst. Leicester, U.K.: Univ. of Leicester, School of Informatics*, Jan. 2020, doi: 10.1109/TFUZZ.2020.2966163.
- [24] S. Wang, J. Sun, I. Mehmood, C. Pan, Y. Chen, and Y. Zhang, "Cerebral micro-bleeding identification based on a nine-layer convolutional neural network with stochastic pooling," *Concurrency Comput., Pract. Exp.*, vol. 32, no. 1, p. e5130, Jan. 2020.
- [25] S. Wang, C. Tang, J. Sun, and Y. Zhang, "Cerebral micro-bleeding detection based on densely connected neural network," *Frontiers Neurosci.*, vol. 13, p. 422, May 2019.
- [26] K. M. Hosny, M. A. Kassem, and M. M. Fouad, "Classification of skin lesions using transfer learning and augmentation with Alex-net," *PLoS ONE*, vol. 14, no. 5, May 2019, Art. no. e0217293.
- [27] M. A. Al-masni, M. A. Al-antari, M.-T. Choi, S.-M. Han, and T.-S. Kim, "Skin lesion segmentation in dermoscopy images via deep full resolution convolutional networks," *Comput. Methods Programs Biomed.*, vol. 162, pp. 221–231, Aug. 2018.
- [28] (2018). *Exchang. Open Neural Network*, ONNX Github Repository. [Online]. Available: <https://github.com/onnx/>
- [29] F. N. Iandola, S. Han, M. W. Moskewicz, K. Ashraf, W. J. Dally, and K. Keutzer, "Squeezenet: Alexnet-level accuracy with 50x fewer parameters and <0.5 MB model size," *ICLR*, 2017, pp. 1–13.
- [30] J. Redmon and A. Farhadi, "YOLO9000: Better, faster, stronger," in *Proc. IEEE Conf. Comput. Vis. Pattern Recognit. (CVPR)*, Jul. 2017, pp. 7263–7271.
- [31] N. Cristianini and J. Shawe-Taylor, *An Introduction to Support Vector Machines and Other Kernel-Based Learning Methods*. Cambridge, U.K.: Cambridge Univ. Press, 2000.
- [32] T. Hastie, R. Tibshirani, and J. Friedman, *The Elements of Statistical Learning: Data Mining, Inference, and Prediction*. Stanford, CA, USA: Springer, Aug. 2009.
- [33] J. S. Suri, "State-of-the-art review on deep learning in medical imaging," *Frontiers Biosci.*, vol. 24, no. 3, pp. 392–426, 2019.
- [34] M. Dorigo, M. Birattari, and T. Stutzle, "Ant colony optimization," *IEEE Comput. Intell. Mag.*, vol. 1, no. 4, pp. 28–39, 2006.
- [35] N. C. F. Codella, D. Gutman, M. E. Celebi, B. Helba, M. A. Marchetti, S. W. Dusza, A. Kallou, K. Liopyris, N. Mishra, H. Kittler, and A. Halpern, "Skin lesion analysis toward melanoma detection: A challenge at the 2017 international symposium on biomedical imaging (ISBI), hosted by the international skin imaging collaboration (ISIC)," in *Proc. IEEE 15th Int. Symp. Biomed. Imag. (ISBI)*, Apr. 2018, pp. 168–172.
- [36] M. A. A. Milton, "Automated skin lesion classification using ensemble of deep neural networks in ISIC 2018: Skin lesion analysis towards melanoma detection challenge," 2019, *arXiv:1901.10802*. [Online]. Available: <http://arxiv.org/abs/1901.10802>
- [37] S. Sreena and A. Lijjya, "Skin lesion analysis towards melanoma detection," in *Proc. 2nd Int. Conf. Intell. Comput., Instrum. Control Technol. (ICICT)*, vol. 1, Jul. 2019, pp. 32–36.
- [38] *The ISIC 2020 Challenge Dataset Skin Lesion Analysis Towards Melanoma Detection*. Accessed: Jun. 29, 2020. [Online]. Available: <https://challenge2020.isic-archive.com/>
- [39] C. Kaul, S. Manandhar, and N. Pears, "FocusNet: An attention-based fully convolutional network for medical image segmentation," 2019, *arXiv:1902.03091*. [Online]. Available: <http://arxiv.org/abs/1902.03091>
- [40] M. K. Hasan, L. Dahal, P. N. Samarakoon, F. I. Tushar, and R. Marti, "DSNet: Automatic dermoscopic skin lesion segmentation," *Comput. Biol. Med.*, vol. 120, May 2020, Art. no. 103738.
- [41] M. A. A. Milton, "Automated skin lesion classification using ensemble of deep neural networks in ISIC 2018: Skin lesion analysis towards melanoma detection challenge," *Auonomous Univ. Barcelona, Barcelona, Spain, Tech. Rep.*, 2019.
- [42] M. A. Al-masni, D.-H. Kim, and T.-S. Kim, "Multiple skin lesions diagnostics via integrated deep convolutional networks for segmentation and classification," *Comput. Methods Programs Biomed.*, vol. 190, Jul. 2020, Art. no. 105351.
- [43] M. A. Kassem, K. M. Hosny, and M. M. Fouad, "Skin lesions classification into eight classes for ISIC 2019 using deep convolutional neural network and transfer learning," *IEEE Access*, vol. 8, pp. 114822–114832, 2020.



**MUHAMMAD ALMAS ANJUM** is currently a Professor at the College of Electrical and Mechanical Engineering, National University of Sciences and Technology (NUST), Pakistan. He has also contributed as a Team Lead in establishing the Centre of Excellence Information Technology, where he served as its first Pioneer Head. He designed and established the Centre of Innovation and Entrepreneurship, College of EME. He has also served as the Dean of the Faculty of Computer Sciences, University of Wah, and the Director of the Research and Development, College of EME, NUST. His areas of specialization are pattern recognition, security systems (biometrics), and computer vision. Apart from this, he has more than 45 international publications in his area of specialization and he has also published a book titled "*Face Recognition a Challenge in Biometrics: Image Resolution Issues in Face Recognition*." He has evaluated more than ten master's and Ph.D. thesis. He is reviewer / member of more than dozen international technical committees as well as an Executive Editor of *UW Journal of Computer Sciences*. He has undertaken different technical projects around the globe while contributing in uplifting the local communities.



**JAVARIA AMIN** actively involved in research and producing high-quality work on medical image processing, pattern recognition, and computer vision. She has published more than 22 research articles in reputed and prestigious international journals with an accumulated impact factor of around 55. Her focus area of research is the detection of anomalies in human body parts using machine learning and powerful deep learning algorithms.



**MUHAMMAD SHARIF** (Senior Member, IEEE) is currently an Associate Professor at COMSATS University Islamabad, Wah Campus, Pakistan. He worked, for one year, at Alpha Soft, an U.K. based software house, in 1995. He is an OCP in Developer Track. He has been in the teaching profession, since 1996. His research interests include medical imaging, biometrics, computer vision, machine learning, and agriculture plants imaging. He also headed the department, from 2008 to 2011, and achieved the targeted outputs. He has more than 210 research publications in IF, SCI, and ISI journals as well as in national and international conferences and gained more than 245 Impact Factor. He has supervised three Ph.D. (CS) and more than 50 M.S. (CS) theses students till date. He received the COMSATS Research Productivity Award, from 2011 to 2018. He served in TPC for the IEEE FIT 2014-2019, and currently serving as an Associate Editor of IEEE ACCESS, a Guest Editor of special issues, and a reviewer of well reputed journals.



**HABIB ULLAH KHAN** (Member, IEEE) received the Ph.D. degree in management information systems from Leeds Beckett University, U.K. He is currently an Associate Professor of MIS at the Department of Accounting & Information Systems, College of Business and Economics, Qatar University, Qatar. He has more than 19 years of industry, teaching, and research experience. He is also an active researcher and his research works are published in leading journals of the MIS field. His research interests include the areas of IT security, online behavior, IT adoption in supply chain management, Internet addiction, mobile commerce, computer mediated communication, IT outsourcing, big data, cloud computing, and e-learning. He is a member of leading professional organizations, like the IEEE, DSI, SWDSI, ABIS, FBD, and EFMD. He is a reviewer of leading journals of his field and also working as an editor for some journals.



**MUHAMMAD SHERAZ ARSHAD MALIK** received the Ph.D. degree from Universiti Teknologi PETRONAS, Malaysia. He has more than ten years of industrial, research, and academia experience in various research and senior administration roles at various countries. He is currently working as an Assistant Professor at the Department of Information Technology, Government College University Faisalabad, Pakistan, where he is also the Chairman of the Department of Estate

Care. His research interests include machine learning and human interaction, data visualization, big data, digital image processing, and artificial intelligence.



**SEIFEDINE KADRY** (Senior Member, IEEE) received the bachelor's degree in applied mathematics from Lebanese University, in 1999, the M.S. degree in computation from Reims University, France, and EPFL, Lausanne, in 2002, the Ph.D. degree from Blaise Pascal University, France, in 2007, and the H.D.R. degree in engineering science from Rouen University, in 2017. He is currently working as an Associate Professor at Beirut Arab University, Lebanon. His current

research interests include education using technology, smart cities, system prognostics, stochastic systems, and probability and reliability analysis. He is a Fellow of IET and ACSIT and a Program Evaluator of ABET. He is an Associate Editor of IEEE ACCESS journal.

• • •